Title
Electroweak Physics at the Tevatron Collider

Author
Aihara, H.

Publication Date
1993-08-01

LBL-34572
UC-414

Lawrence Berkeley Laboratory
UNIVERSITY OF CALIFORNIA

Physics Division

Presented at the Thirteenth International Conference on
Physics in Collision, Heidelberg, Germany, June 16–18, 1993,
and to be published in the Proceedings

Electroweak Physics at the Tevatron Collider

H. Aihara

August 1993

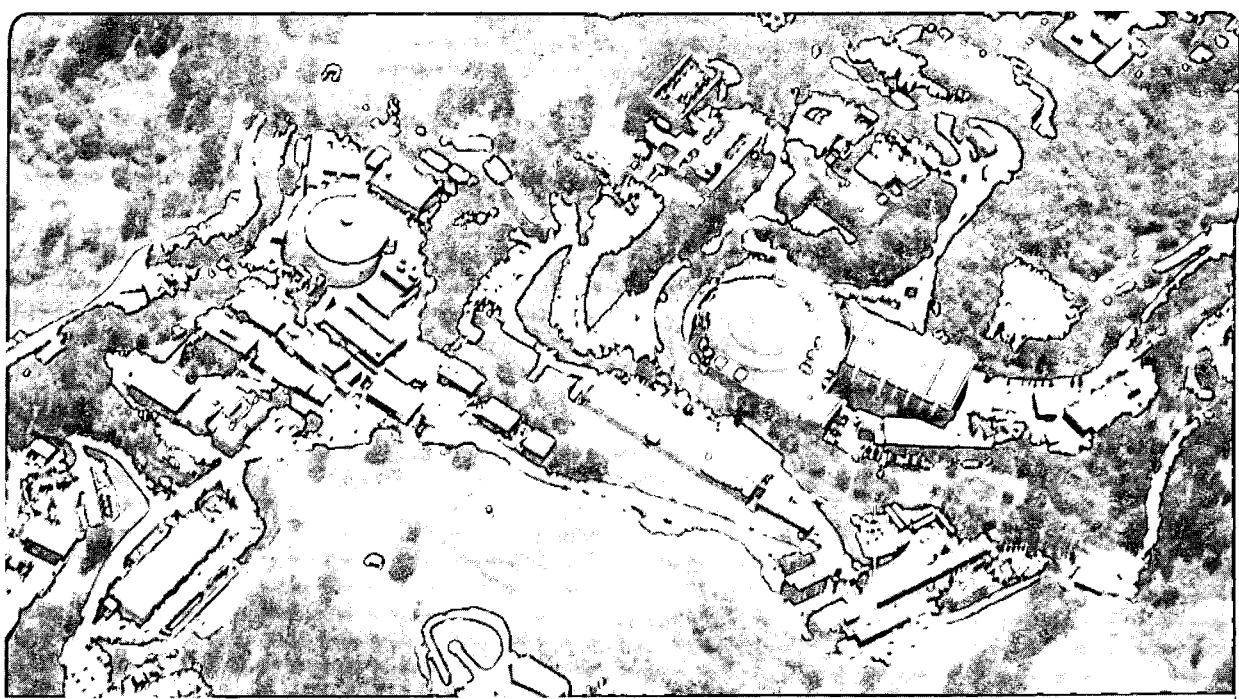

Prepared for the U.S. Department of Energy under Contract Number DE-AC03-76SF00098

DISCLAIMER

LBL-34572

ELECTROWEAK PHYSICS AT THE TEVATRON COLLIDER

Hiroaki Aihara
Physics Division
Lawrence Berkeley Laboratory
Berkeley, California 94720

This work was supported by the Director, Office of Energy Research, Office of High Energy and Nuclear Physics, Division of High Energy Physics of the U.S. Department of Energy, under Contract No.DE-AC03-76SF00098.

ELECTROWEAK PHYSICS AT THE TEVATRON COLLIDER

Hiroaki Aihara
Lawrence Berkeley Laboratory
Berkeley, California 94720

Abstract

Preliminary results on electroweak physics from the 1992-1993 run with the CDF and DØ detectors at the Tevatron collider are presented. New measurements of the ratio of the W and Z production cross sections times the branching fractions for subsequent decay into leptons are shown. The W width, $\Gamma(W)$, and a limit on the top-quark mass independent of decay mode are extracted. The status of a measurement of the charge asymmetry of electrons from W decay is given. Also shown are a study of diboson ($W\gamma$, $Z\gamma$ and WZ) production and a search for a new neutral gauge boson (Z').

Presented at
XIII INTERNATIONAL CONFERENCE ON PHYSICS IN COLLISION,
Heidelberg, Germany, June 16-18, 1993,
and to be published in the Proceedings.

1 Introduction

The Tevatron $\bar{p}p$ collider at Fermilab completed a very successful yearlong run at the end of May, 1993. CDF[1] collected a total of ~ 22 pb^{-1} of data, about 5 times more than the data collected during the 1988-1989 run. DØ[2] completed its first data-taking run and collected a total of ~ 16 pb^{-1}. We present preliminary results on 1) a measurement of the ratio $\sigma(\bar{p}p \to WX)Br(W \to \ell\nu)/\sigma(\bar{p}p \to ZX)Br(Z \to \ell\ell)$ ($\ell = e, \mu$), 2) a measurement of the charge asymmetry of electrons from W decay, 3) a study of diboson ($W\gamma$, $Z\gamma$ and WZ) production, and 4) a search for a new neutral gauge boson (Z').

2 The CDF and DØ Detectors

The CDF and DØ detectors are described in detail in Refs.[3] and [4], respectively. Here we briefly describe the detector components most relevant to the analysis presented here. The CDF detector consists of the central tracking system, the calorimeter system and the muon system. The major component of the CDF central tracking system is a 1.3 m radius tracking chamber contained in a solenoidal 1.41 T magnet. The momentum resolution is $\delta p_{\rm T}/p_{\rm T} = 0.0011 p_{\rm T}$ ($p_{\rm T}$ in GeV/c). Outside the solenoid is the central ($|\eta| < 1.1$)[1] calorimeter, which has an electromagnetic section made of lead-scintillator and a hadronic section of iron-scintillator. A proportional chamber (strip chamber) imbedded at electromagnetic shower maximum measures the position and the shape of electromagnetic showers. The transverse segmentation of projective towers is $0.1 \times 15°$ in η and ϕ. The electromagnetic section has an energy resolution[2] of $(13.5\%/\sqrt{\rm E}) \oplus 2\%$ (E is in GeV) and the hadronic section has an energy resolution of $(75\%/\sqrt{\rm E}) \oplus 3\%$ for isolated pions. Outside of the central calorimeter in the region of $|\eta| < 0.61$ are muon drift chambers. The forward region is covered by the plug ($1.1 < |\eta| < 2.2$) and forward ($2.2 < |\eta| < 4.2$) gas-sampling calorimeters.

The DØ detector consists of the non-magnetic central tracking system, the calorimeter system and the muon system. The calorimeter system consists of uranium-liquid argon sampling detectors contained in a central and two end cryostats and the inter-cryostat detectors made of scintillator tiles, providing the η coverage of $|\eta| \leq 4.4$. Its electromagnetic section has an energy resolution of $15\%/\sqrt{\rm E}$, while the hadronic section has an energy resolution of $50\%/\sqrt{\rm E}$ for isolated pions. The transverse segmentation is 0.1×0.1 in η and ϕ. In the third longitudinal section

[1] This η is a pseudorapidity defined as $\eta = -ln(tan\frac{\theta}{2})$, where θ is the polar angle from the beam axis with respect to the detector origin which can be significantly different from the event origin due to a large spread ($\sigma_z \sim 30cm$) of the interaction region.

[2] The symbol $\oplus$ denotes a quadratic sum.

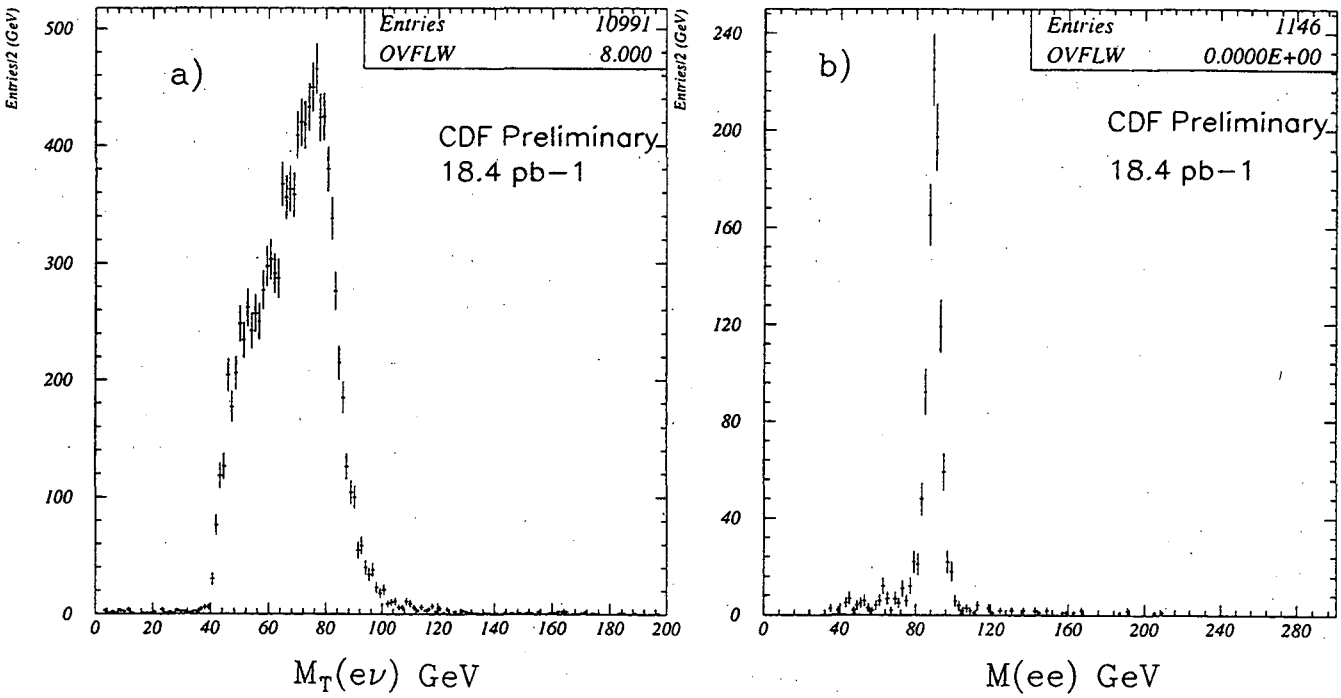

Figure 1: (a) Transverse mass distribution for $W \rightarrow e\nu$ events and (b) Invariant mass distribution for $Z \rightarrow ee$ events from CDF.

of an electromagnetic module the transverse segmentation is doubled in both directions to 0.05×0.05. The muon system has magnetized iron toroids between the first two of three muon drift tube layers, providing the η coverage of $|\eta| \leq 3.3$. The current momentum resolution, $\delta p/p \geq 0.2$, is dominated by the uncertainty in the alignments of drift tube layers.

3 W and Z events from 1992-1993 run

In both CDF and DØ the $W \rightarrow e(\mu)\nu$ and $Z \rightarrow ee(\mu\mu)$ samples were selected from a sample of events with at least one well-measured, isolated electron (muon) with transverse momentum greater than 20 GeV/c. W candidates were obtained by requiring a large missing transverse energy ($\not\!\!E_T > 20$ GeV), while Z candidates required the presence of a second electron (or muon) satisfying looser offline cuts.

In CDF an electron sample was selected from events passing a hardware trigger requiring an electromagnetic cluster with $E_T > 12$ GeV in the central calorimeter, a ratio of hadronic to electromagnetic E_T in the cluster < 0.125 and a track associated with this cluster with $p_T > 6$ GeV/c measured by the hardware track processor. The offline selection requires at least one central ($|\eta| < 1.1$) electron, satisfying the following 5 criteria: 1) an isolation variable, $I = (E_T(R < 0.4) - E_T(\text{cluster}))/E_T(\text{cluster}) < 0.1$, where $E_T(\text{cluster})$ is the transverse energy in the electron cluster and $E_T(R < 0.4)$ is the transverse energy within a cone of radius $R = \sqrt{\Delta\eta^2 + \Delta\phi^2} = 0.4$ centered

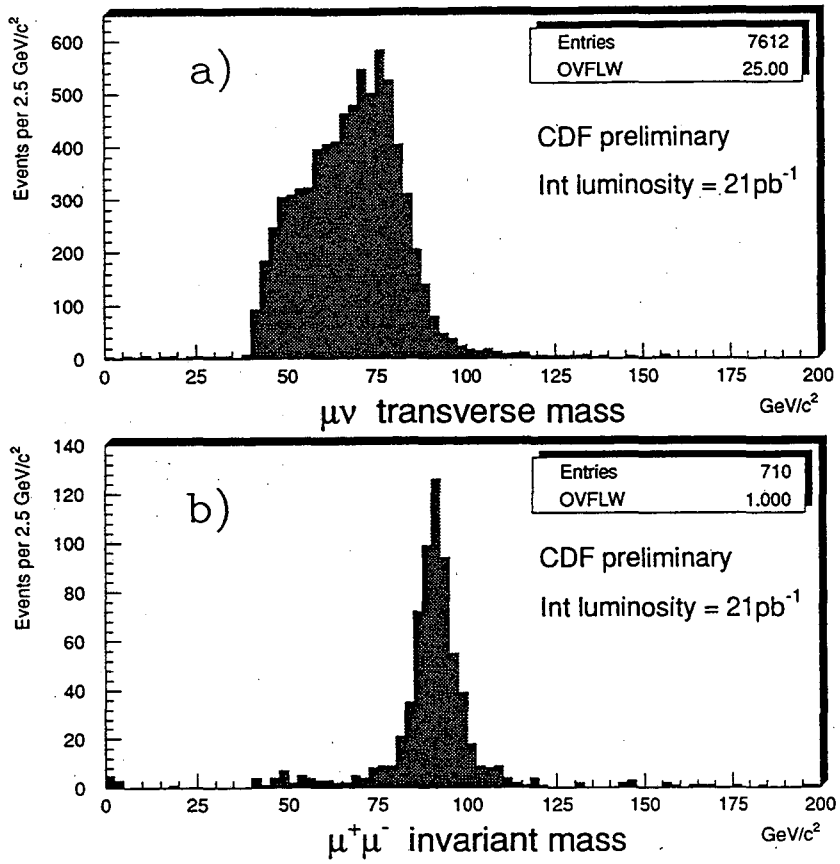

Figure 2: (a) Transverse mass distribution for $W \rightarrow \mu\nu$ events and (b) Invariant mass distribution for $Z \rightarrow \mu\mu$ events from CDF.

on the electron cluster; 2) HAD/EM $<$ 0.055 + 0.045 $\times$ E(cluster)/100, where HAD(EM) is the energy in the hadronic (electromagnetic) section of the calorimeter and E(cluster) is the energy of the electron cluster in GeV; 3) the strip-chamber shower profile and the lateral energy sharing between calorimeter towers are consistent with an electron; 4) the ratio of cluster energy to track momentum, $E/p < 1.5$; and, 5) there is a good match between the strip-chamber shower and the extrapolated track position positions. Z candidates were selected by requiring that there be a second electromagnetic cluster in the region of $|\eta| < 2.4$ with $E_T > 10$ GeV, $I < 0.1$ and HAD/EM < 0.1. In addition, if this cluster is in the central region $E/p < 2.0$ and if the cluster is in the plug or forward region the transverse profile must be consistent with an electron shower. The transverse mass (M_T) distribution for $W \rightarrow e\nu$ and the invariant mass distribution for $Z \rightarrow ee$ based on an integrated luminosity of 18.4 pb^{-1} are shown in Fig. 1. Here, M_T is defined as $M_T = \sqrt{2E_T \not\!\!E_T(1 - \cos\phi^{e\nu})}$ and $\phi^{e\nu}$ is the azimuthal angle between the electron and $\not\!\!E_T$ vector.

A muon trigger is formed when hits in the muon chambers match a track with $p_T > 9$ GeV/c found by the hardware track processor. A muon data sample was selected from the muon-triggered events with at least one muon track in the region of $|\eta| < 0.61$, satisfying the following criteria: 1) the muon track reconstructed in the central tracker matches a track segment in the muon chambers to better than 2 cm in $r\phi$-plane; 2) the muon track points at a calorimeter tower with less than

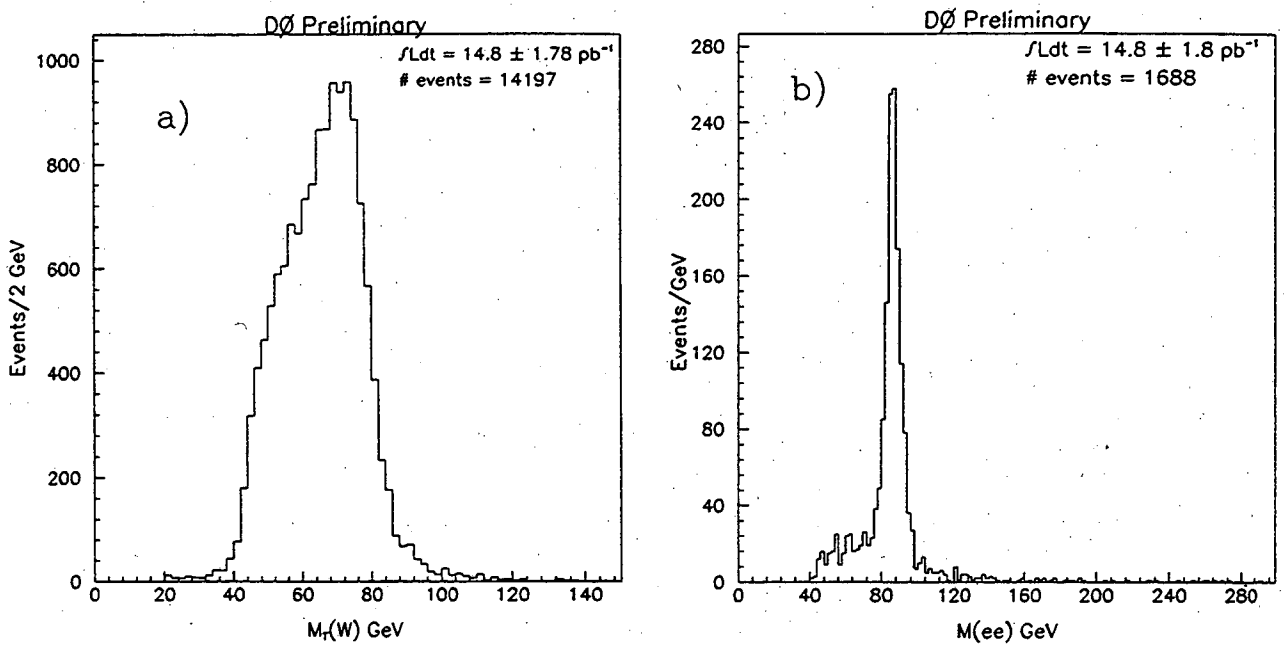

Figure 3: (a) Transverse mass distribution for $W \rightarrow e\nu$ events and (b) Invariant mass distribution for $Z \rightarrow ee$ events from DØ.

6 GeV of energy in the hadronic section and 2 GeV in the electromagnetic section; and, 3) $I = (\mathrm{E_T}(\mathrm{R} < 0.4) - \mathrm{E_T})/p_\mathrm{T} < 0.1$, where $\mathrm{E_T}$ is the transverse energy in the calorimeter tower traversed by the track, $\mathrm{E_T}(\mathrm{R} < 0.4)$ is the transverse energy in a cone of radius 0.4 around the track and p_T is the transverse momentum measured by the central tracker. Z candidates must have a second minimum ionizing track with $|\eta| < 1.0$ and $p_\mathrm{T} > 20$ GeV. The transverse mass distribution for $W \rightarrow \mu\nu$ and the invariant mass distribution for $Z \rightarrow \mu\mu$ based on an integrated luminosity of 21 pb^{-1} are shown in Fig. 2.

In DØ an electron data sample was selected from events passing a single-electron trigger requiring one electron with $\mathrm{E_T} > 20$ GeV satisfying shower shape and isolation cuts imposed in the third level of the trigger logic. The offline selection requires at least one electron in the region of $|\eta| < 1.1$ and $1.5 < |\eta| < 3.2$, satisfying the following criteria: 1) the ratio of the electromagnetic energy to the total shower energy is greater than 0.9; 2) the lateral and longitudinal shower shapes are consistent with an electron; 3) $I = (\mathrm{E}(\mathrm{R} < 0.4) - \mathrm{E_{EM}}(\mathrm{R} < 0.2))/\mathrm{E_{EM}}(\mathrm{R} < 0.2) < 0.15$, where $\mathrm{E}(\mathrm{R} < 0.4)$ is the total shower energy within a cone of radius 0.4 and $\mathrm{E_{EM}}(\mathrm{R} < 0.2)$ is the electromagnetic energy within a cone of 0.2; and, 4) the cluster has a track with a good match between the cluster position measured by the calorimeter and the extrapolated track position. For Z candidates the presence of a second electromagnetic cluster which passes the cuts $1 - 3$ is required. The transverse mass distribution for $W \rightarrow e\nu$ and the invariant mass distribution for $Z \rightarrow ee$, based on an integrated luminosity of 14.8 pb^{-1} are shown in Fig. 3.

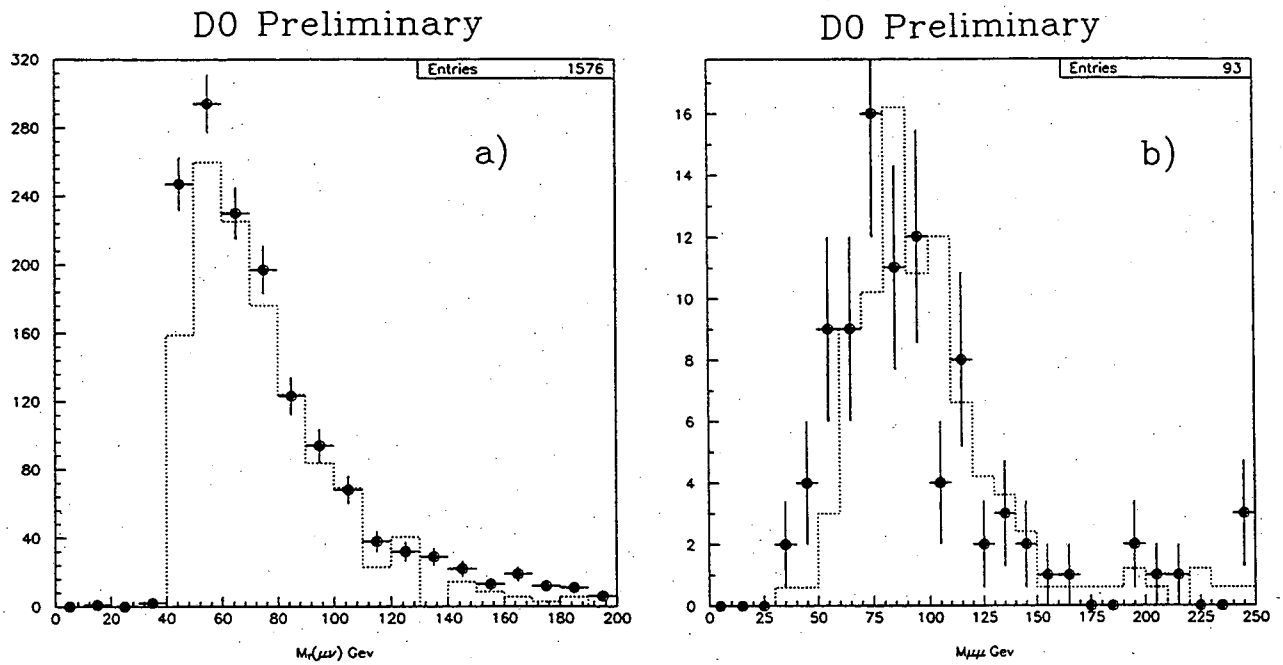

Figure 4: (a) Transverse mass distribution for $W \rightarrow \mu\nu$ events and (b) Invariant mass distribution for $Z \rightarrow \mu\mu$ events from DØ. In both figures the points are the data and the dotted line is the Monte Carlo prediction for the signal.

The muon trigger has 3 decision levels which accept single muons with $p_T >$ 15 GeV/c. A muon sample was obtained by requiring at least one muon track in the region of $|\eta| < 1.7$, satisfying the following cuts: 1) the muon track has a good overall track fit in the muon system; 2) the muon track has good track segments before and after the iron toroids; 3) the muon track has a minimum path-length through the magnetized iron toroid of $\int B d\ell > 2.0$ Tm; 4) there is at least one track in the central drift chamber matching the muon track within $\delta\phi < 0.25$ and $\delta\theta < 0.30$ radians; 5) the muon track passes a global χ^2 cut including the information from the central drift chamber; 6) the muon track has an energy deposition greater than 1 GeV in the calorimeter towers within a cone of radius 0.2 around the muon track; 7) $I = (\text{E(observed)} - \text{E(MIP)})/\delta\text{E(MIP)} < 3$, where E(observed) is the energy in the calorimeter tower hit by the muon track and 5×5 towers around the track (corresponding to a cone of radius ~ 0.2), E(MIP) is the expected contribution from the muon ionization and δE(MIP) is the expected error on E(MIP); and, 8) the muon track satisfies impact parameter cuts (at the event vertex) of $\delta(xy) < 10$ cm and $\delta(rz) < 25$ cm. The Z sample was selected requiring a second muon track with $p_T > 15$ GeV/c which satisfies only the first cut and $|\Delta\phi| \leq 160°$ and $|\Delta\theta| \leq 170°$ between both muon tracks to reduce cosmic rays. The transverse mass distribution for $W \rightarrow \mu\nu$ and the invariant mass distribution for $Z \rightarrow \mu\mu$ based on an integrated luminosity of 7.3 pb^{-1}, corresponding to $\sim 1/2$ of the full data set, are shown in

Fig. 4 with the Monte Carlo predictions superimposed. The Monte Carlo predictions were normalized to the number of W and Z candidates after background subtraction.

4 The Ratio $\sigma Br(W \to \ell\nu)/\sigma Br(Z \to \ell\ell)$

The ratio of the W and Z production cross sections times the branching fractions for subsequent decay into leptons can be expressed as

$$R = \frac{\sigma(\bar{p}p \to WX)Br(W \to \ell\nu)}{\sigma(\bar{p}p \to ZX)Br(Z \to \ell\ell)} = \frac{\sigma(\bar{p}p \to WX)}{\sigma(\bar{p}p \to ZX)} \times \frac{\Gamma(W \to \ell\nu)}{\Gamma(W)} \times \frac{\Gamma(Z)}{\Gamma(Z \to \ell\ell)}$$

Most of the theoretical and experimental systematic uncertainties cancel in this ratio, allowing a precise determination of the W width and constraining the possibility of non-standard decay modes of the W. In particular, the result can be used to set a limit on the top quark mass independent of decay mode.

Using experimentally measured quantities R can be written as

$$R = \frac{N_W - B_W}{N_Z - B_Z} \frac{A_Z}{A_W} \frac{\epsilon_Z}{\epsilon_W},$$

where N_W and N_Z are the number of W and Z candidates, B_W and B_Z are the estimated backgrounds in W and Z samples, A_W and A_Z are the geometric and kinematic acceptances, and ϵ_W and ϵ_Z are the detection efficiencies. CDF observed 10991 $W \to e\nu$ and 1053 $Z \to ee$ candidates from the 18.4 pb^{-1} data sample. Table 1 summarizes the analysis of this data sample. The background for $W \to e\nu$ includes contributions from QCD processes, $W \to \tau\nu$ followed by $\tau \to e\nu\nu$, $Z \to ee$ where one of the electrons is lost and $Z \to \tau\tau$ where one τ decays into an electron and two neutrinos, resulting in a large $\not\!\!E_T$. The background for $Z \to ee$ is dominated by QCD processes. The acceptance includes geometric and kinematic cuts described above. The efficiency includes efficiencies for the trigger and offline cuts. A multiplicative factor of 1.01 ± 0.01 is used to correct $Z \to ee$ yield for Drell-Yan contribution and Z width effect[5]. CDF obtains the ratio

$$R_e \equiv \frac{\sigma Br(W \to e\nu)}{\sigma Br(Z \to ee)} = 10.65 \pm 0.36(\text{stat.}) \pm 0.27(\text{sys.}).$$

Results from DØ reported here are based on a partial data set. The electron analysis is based on the 3.45 pb^{-1} data sample and tighter kinematic cuts than ones described above. DØ observed 2824 $W \to e\nu$ with kinematic cuts of $E_T > 25$ GeV on the electron and $\not\!\!E_T > 25$ GeV and 172 $Z \to ee$ candidates after requiring $E_T > 25$ GeV and all offline cuts on both electrons. Table 2 summarizes results from DØ in the electron channel. The acceptance includes geometric and

Table 1: Summary of CDF $W \to e\nu$ and $Z \to ee$ analysis

Channel	$W \to e\nu$	$Z \to ee$
Candidates	10991	1053
Background	1175^{+121}_{-99}	52 ± 9
Signal	$9816 \pm 105 \pm 106$	$1001 \pm 32 \pm 9$
Acceptance	0.338 ± 0.006	0.372 ± 0.006
Efficiency	0.749 ± 0.013	0.731 ± 0.015

Table 2: Summary of DØ $W \to e\nu$ and $Z \to ee$ analysis

Channel	$W \to e\nu$	$Z \to ee$
Candidates	2824	172
Background	102 ± 31	18 ± 5
Signal	$2722 \pm 54 \pm 31$	$154 \pm 14 \pm 5$
Acceptance	0.51 ± 0.04	0.42 ± 0.04
Efficiency	0.63 ± 0.05	0.46 ± 0.07

kinematic cuts, while the efficiency includes efficiencies for the trigger and offline cuts. DØ obtains values for the production cross section times branching fraction of $\sigma Br(W \to e\nu) = 2.48 \pm 0.05(\text{stat.}) \pm 0.26(\text{sys.}) \pm 0.30(\text{LUM})$[3] nb and $\sigma Br(Z \to ee) = 0.235 \pm 0.019(\text{stat.}) \pm 0.040(\text{sys.}) \pm 0.028(\text{LUM})$ nb, resulting in

$$R_e = 10.55 \pm 0.87(\text{stat.}) \pm 1.07(\text{sys.}).$$

The muon analysis is based on the data sample of 7.3 pb^{-1} for $|\eta| \leq 1$ and 5.9 pb^{-1} for $1 \leq |\eta| \leq 1.7$, resulting in 1576 $W \to \mu\nu$ and 93 $Z \to \mu\mu$ candidates. A summary of the muon analysis is shown in Table 3. The background to the $Z \to \mu\mu$ sample at DØ is primarily from cosmic rays and fake tracks due to false hits in the muon chambers. Unlike the electron analysis the acceptance shown here includes the trigger efficiency in addition to kinematic and geometric cuts. The values of the production cross section times branching fraction are $\sigma Br(W \to \mu\nu) = 2.00 \pm 0.07(\text{stat.}) \pm 0.41(\text{sys.}) \pm 0.24(\text{LUM})$ nb and $\sigma Br(Z \to \mu\mu) = 0.20 \pm 0.02(\text{stat.}) \pm 0.05(\text{sys.}) \pm 0.02(\text{LUM})$ nb, resulting in

$$R_\mu = 10.0 \pm 1.1(\text{stat.}) \pm 2.4(\text{sys.}).$$

[3]LUM denotes the error due to uncertainty in the luminosity measurement.

Table 3: Summary of DØ $W \to \mu\nu$ and $Z \to \mu\mu$ analysis

Channel	$W \to \mu\nu$	$Z \to \mu\mu$
Candidates	1576	93
Background	$378 \pm 20 \pm 62$	$6 \pm 2 \pm 3$
Signal	$1198 \pm 44 \pm 62$	$87 \pm 10 \pm 3$
Acceptance	0.15 ± 0.01 ($\|\eta\| \leq 1$) 0.024 ± 0.01 ($1 \leq \|\eta\| \leq 1.7$)	0.12 ± 0.01 ($\|\eta\| \leq 1$) 0.03 ± 0.01 ($1 \leq \|\eta\| \leq 1.7$)
Efficiency	0.495 ± 0.092	0.428 ± 0.099

Combining R_e and R_μ assuming the $e - \mu$ universality, DØ obtains the result:

$$R \equiv \frac{\sigma Br(W \to \ell\nu)}{\sigma Br(Z \to \ell\ell)} = 10.43 \pm 1.23(stat. \oplus sys.),$$

where ℓ is e or μ. These results on R from CDF and DØ are shown in Fig. 5 together with previously published results[6]. The average over all measurements (World Average) including new results from CDF and DØ gives $R = 10.38 \pm 0.32$ (*stat.* and *sys.* combined).

The W width, $\Gamma(W)$, can be extracted from a measurement of R as

$$\Gamma(W) = \frac{\sigma(\bar{p}p \to W)}{\sigma(\bar{p}p \to Z)} \times \frac{\Gamma(W \to \ell\nu)}{\Gamma(Z \to \ell\ell)} \times \Gamma(Z) \times R^{-1}.$$

Both CDF and DØ use a theoretical calculation of $\Gamma(W \to \ell\nu)/\Gamma(Z \to \ell\ell) = 2.70 \pm 0.02$[7] and the LEP measurement of the $\Gamma(Z) = 2.487 \pm 0.010$ GeV/c^2[8]. The major theoretical error on the W and Z production cross sections comes from their structure function dependence and the uncertainty in the ratio of parton density functions (PDFs) for down and up valence quarks. CDF uses the theoretical calculation of $\sigma_W/\sigma_Z = 3.23 \pm 0.03$ by Martin, Stirling and Roberts[9]. This relative error of about 1%(= 0.03/3.23) results in a $\sim$ 20 MeV/c^2 uncertainty on $\Gamma(W)$. DØ estimates $\sigma_W/\sigma_Z = 3.26 \pm 0.08$ using the calculation of Hamberg, van Neerven and Matsuura[10], convoluted with PDFs consistent with a measurement of F_2^n/F_2^p from NMC[11]. Its relative error of about 2.5%(= 0.08/3.26) results in a $\sim$ 50 MeV/c^2 uncertainty on $\Gamma(W)$. From the above values we obtain

$$\begin{aligned}
\Gamma(W) &= 2.033 \pm 0.069(stat.) \pm 0.057(sys.)\ \text{GeV/c}^2 \quad \text{CDF } e \\
&= 2.08 \pm 0.25(stat. \oplus sys.)\ \text{GeV/c}^2 \quad \text{DØ } e\mu \text{ combined} \\
&= 2.089 \pm 0.031(stat. \oplus sys.)\ \text{GeV/c}^2 \quad \text{World Average}
\end{aligned}$$

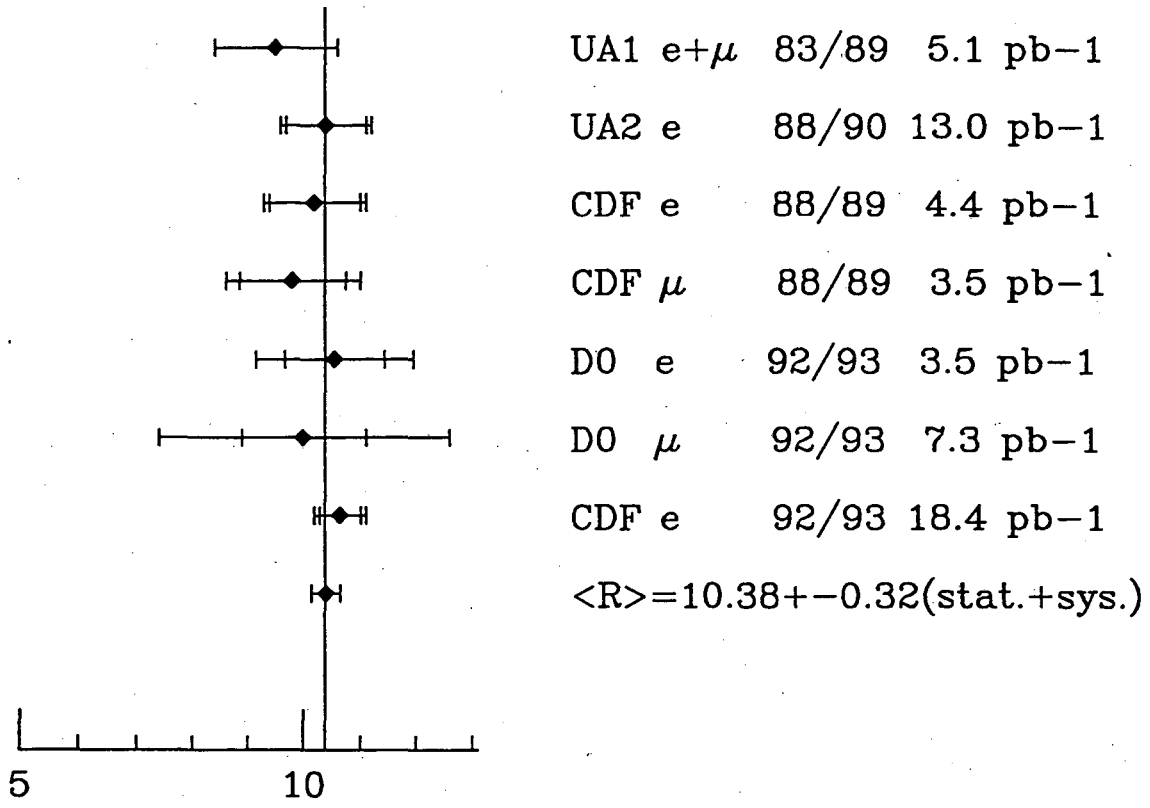

Figure 5: Compilation of $R = \sigma Br(W \to \ell\nu)/\sigma Br(Z \to \ell\ell)$ measurements.

The results can be compared with the Standard Model prediction[12] of $\Gamma(W) = 2.08 \pm 0.02$ GeV/c^2 for $M(t) > M(W) - M(b)$, where $M(t)$, $M(W)$ and $M(b)$ are the masses of the top quark, the W boson and the b quark, respectively. In order to set a limit on the top quark mass (for $M(t) < M(W) - M(b)$) independent of the decay modes of the top quark, we use the ratio $\Gamma(W)/\Gamma(W \to \ell\nu)$ instead of $\Gamma(W)$ itself because this ratio is less sensitive to the value of the W mass. Figure 6 shows a prediction for the ratio $\Gamma(W)/\Gamma(W \to \ell\nu)$ as a function of the top quark mass [12, 13]. From the values quoted above and $\Gamma(Z \to \ell\ell) = 83.24 \pm 0.42$ MeV/c^2[8] we find

$$\begin{aligned} \Gamma(W)/\Gamma(W \to \ell\nu) &= 9.09 \pm 0.30(stat.) \pm 0.26(sys.) \text{ CDF } e \\ &= 9.3 \pm 1.1(stat. \oplus sys.) \text{ DØ } e\mu \text{ combined} \\ &= 9.28 \pm 0.246(stat. \oplus sys.) \text{ World Average} \end{aligned}$$

The corresponding lower limits on the top quark mass at 95% confidence level are:

$$\begin{aligned} M(t) &> 62 \text{ GeV/c}^2 \text{ CDF } e \\ &> 43 \text{ GeV/c}^2 \text{ DØ } e\mu \text{ combined} \\ &> 62 \text{ GeV/c}^2 \text{ World Average} \end{aligned}$$

The World Average does not improve the limit on $M(t)$ over that from the 1992-1993 CDF electron measurement alone. This is because the World Average value

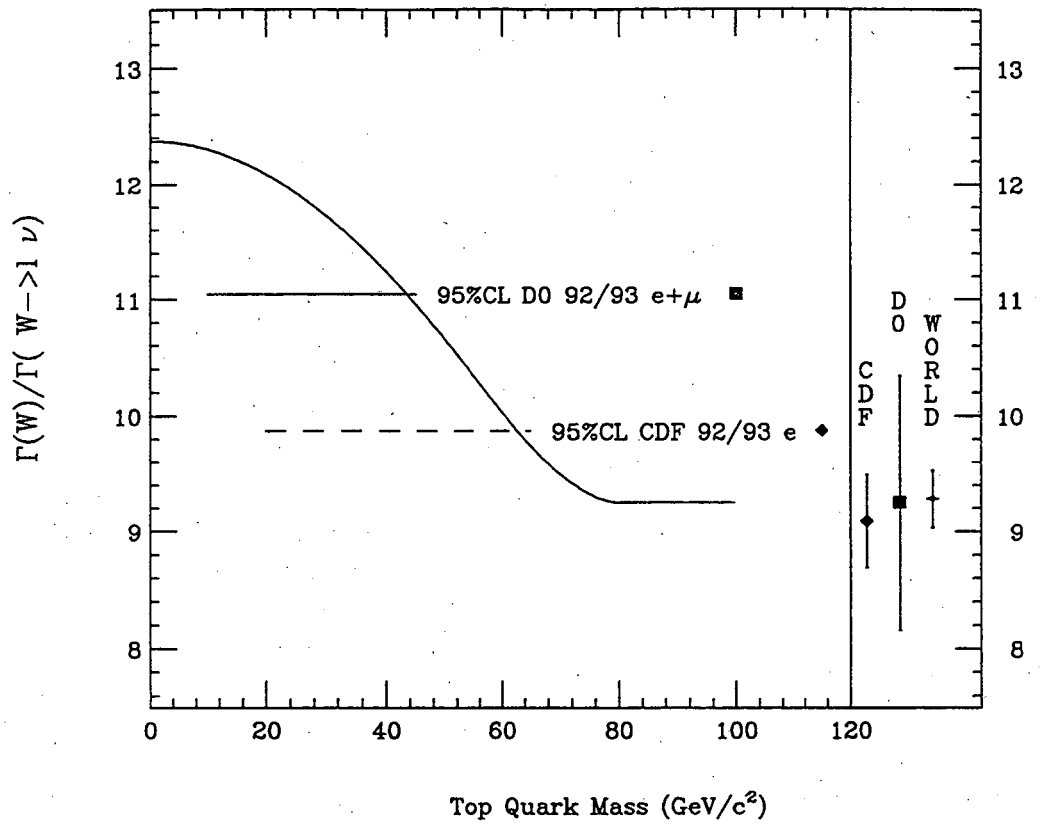

Figure 6: The ratio $\Gamma(W)/\Gamma(W \to \ell\nu)$ as a function of the top quark mass for $M_W = 80.0$ GeV/c^2 and $\alpha_s = 0.13$. Also shown are preliminary measurements and the 95% C.L. limits from CDF and DØ and the average over all measurements.

of $\Gamma(W)/\Gamma(W \to \ell\nu)$ is larger than that of the 1992-1993 electron result from CDF (though the error is smaller).

5 The charge asymmetry of electrons from W decay

The W production in $\bar{p}p$ collisions at $\sqrt{s} = 1.8$ TeV is dominantly from a valence-valence or valence-sea quark-antiquark interaction. Therefore a $W^+(W^-)$ is produced primarily by the interaction of a $u(d)$ quark from the proton and a $\bar{d}(\bar{u})$ quark from the antiproton. In the proton the u valence quark momentum distribution, $u(x)$, is harder than the d valence quark distribution, $d(x)$ [13, 14] and, therefore, a $W^+(W^-)$ is produced with a boost in the proton (antiproton) direction. A measurement of the W^+ and W^- rapidity distributions (Y_{W+-}) gives the information on PDFs in the region of low x and high $q^2(\sim M_W^2)$ where Ws and Zs are produced [13, 14]. Because there is a twofold ambiguity in reconstructing Y_W in a $W \to \ell\nu$ decay (due to the fact that the component of neutrino momentum along the beam direction is not measured) we measure the Y_W distribution indirectly via the charged lepton rapidity distribution (Y_ℓ), which is a sum of the W rapidity and the lepton rapidity ($Y_\ell^{\rm CM}$) in the W rest frame: $Y_{\ell+} = Y_{W+} + Y_{\ell+}^{\rm CM}$, where $Y_\ell^{\rm CM}$

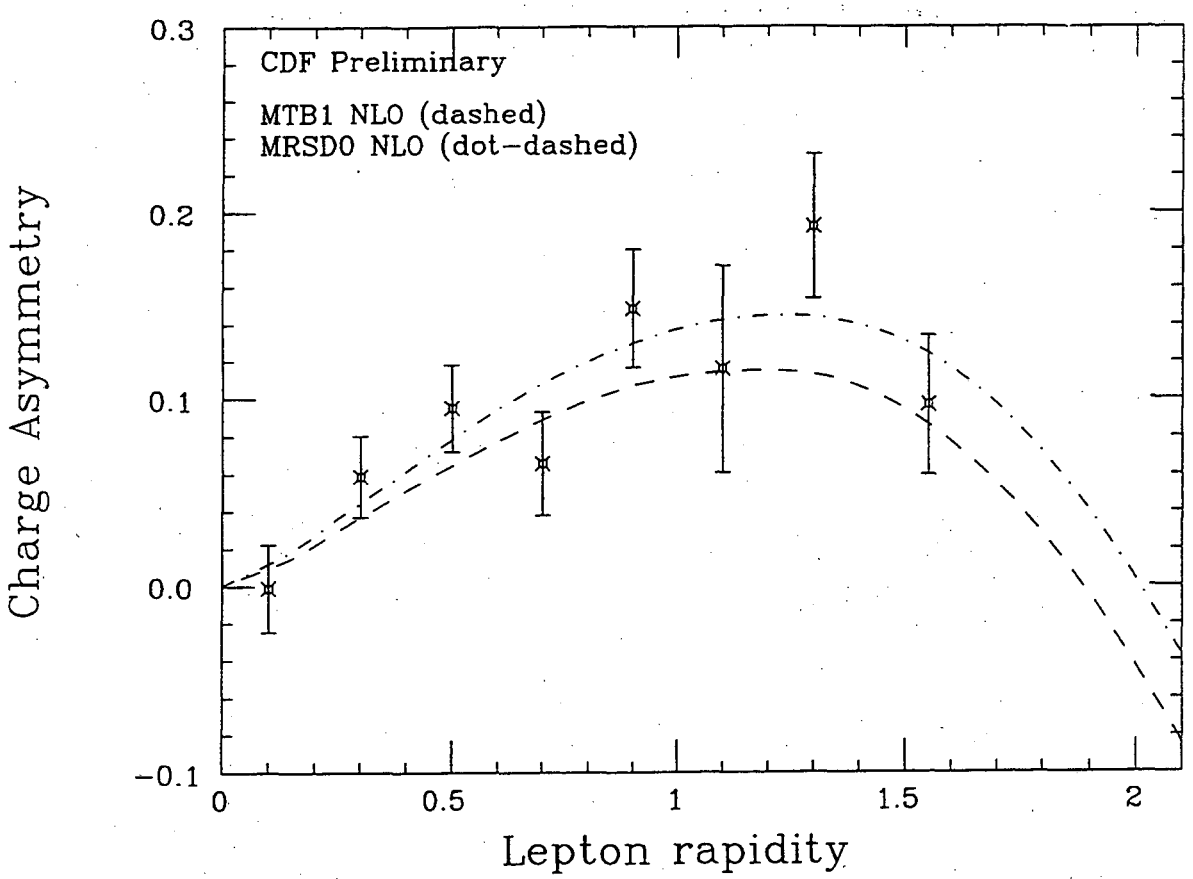

Figure 7: Charge asymmetry in $W \to e\nu$ events from CDF. Superimposed with the data points are the predictions of MTB1 NLO (dashed) and MRSD0 NLO (dot-dashed) parton density functions.

is determined by the $V-A$ couplings. At $\sqrt{s} = 1.8$ TeV the asymmetry due to $u(x)$ and $d(x)$ is larger than that from the $V-A$ effect and of the opposite sign. The experimentally convenient quantity is the charge asymmetry of the leptons as a function of pseudorapidity (corrected for the z position of the event vertex),

$$A(\eta) \equiv \frac{d\sigma(\ell^+)/d\eta - d\sigma(\ell^-)/d\eta}{d\sigma(\ell^+)/d\eta + d\sigma(\ell^-)/d\eta},$$

because it is insensitive to acceptance corrections. Furthermore, because $A(-\eta) = -A(\eta)$ by CP invariance the result can be shown as $|A(\eta)|$ plotted against $|\eta|$. Figure 7 shows a preliminary result from CDF on the asymmetry with two different PDFs superimposed. The result is based on the ~ 10 pb^{-1} $W \to e\nu$ data, corresponding to $\sim 1/2$ of the full data sample from the 1992-1993 run. For this analysis CDF includes electrons detected in the plug calorimeter, extending the η coverage for electrons to $|\eta| = 1.7$. A measurement of $A(\eta)$ with this η coverage will provide information about PDFs in the region of $x \sim 0.007 - 0.24$. Efforts to include the full data sample and to discriminate between various PDFs are in progress.

6 A study of diboson ($W\gamma$, $Z\gamma$ and WZ) productions

Direct measurements of the trilinear couplings ($WW\gamma$ and WWZ) of the electroweak gauge bosons are possible by detecting diboson production such as $W\gamma$, $Z\gamma$, W^+W^- and WZ at Tevatron. In the Standard Model the $WW\gamma$ vertex is uniquely determined by the the $SU(2)_L \otimes U(1)_Y$ gauge symmetry. With the assumption of CP-invariance there are two parameters (κ and λ) to describe the $WW\gamma$ vertex. These parameters are related to the magnetic dipole (μ_W) and electric quadrupole (Q_W) moments of the W boson: $\mu_W = \frac{e}{2M_W}(1+\kappa+\lambda)$, $Q_W = -\frac{e}{M_W^2}(\kappa-\lambda)$. In the Standard Model the values for κ and λ are fixed: $\kappa = 1, \lambda = 0$. Significantly different values of κ and λ result in an increase of the production cross section of the $W\gamma$ events. The UA2 experiment published the first direct measurement of κ and λ based on 13 pb^{-1} data at $\sqrt{s} = 630$ GeV[15]. The $Z\gamma$ production process does not probe trilinear coupling in the Standard Model, but is sensitive to non-standard interactions that might arise, for example, if the gauge bosons are composite. The W^+W^- and WZ production processes are also of interest because there are important cancellations in the amplitudes of these processes which rely on the gauge structure of the WWZ trilinear coupling. In the following we present preliminary results from CDF on measurements of the production cross sections times branching fractions for $W\gamma$ and $Z\gamma$ in the electron and muon channels using the 1988-1989 data and preliminary results from DØ on a search for $W\gamma$ in the electron channel using the 1992-1993 data. In addition, the status of a search for WZ pairs at CDF is mentioned briefly.

CDF searched for the $W\gamma$ and $Z\gamma$ events using the 1988-1989 electron and muon W and Z data samples, corresponding to an electron data of $\int Ldt = 4.05 \pm 0.28$ pb^{-1} and a muon data of $\int Ldt = 3.54 \pm 0.24$ pb^{-1}. The selection criteria for the W and Z samples are described earlier. Candidates were obtained by requiring an additional well-measured and isolated photon with $E_T > 5$ GeV in the central calorimeter ($|\eta_\gamma| < 1.1$) satisfying the following criteria: $E_T(R < 0.4) - E_T^\gamma < 2.0$ GeV; the sum of the transverse momenta of charged tracks within a cone of radius 0.4 centered on a photon $\Sigma p_T(R < 0.4) < 2.0$ GeV; no 3-D tracks pointing at the EM cluster; electromagnetic energy fraction of the EM cluster consistent with a photon; transverse shower shape in the central electromagnetic calorimeter towers consistent with test-beam electrons; transverse shape in the strip chamber consistent with photons; no other clusters of energy > 1.0 GeV in the strip chamber within the EM cluster, and an angular separation between the W/Z decay lepton(s) and the photon $\Delta R_{\ell\gamma} > 0.7$. The $\Delta R_{\ell\gamma} > 0.7$ cut suppresses the contribution of radiative decays in the signal. The overall efficiency for finding photons was determined to be $\epsilon_\gamma = 0.80 \pm 0.01$. CDF observed 8(5) electron(muon) $W\gamma$ and 2(2) electron(muon) $Z\gamma$ candidates.

Table 4: Summary of $W\gamma$ and $Z\gamma$ results from CDF. The first error is statistical and the second systematic.

Channel	Candidates	Background	Signal	SM prediction
$W(e\nu)\gamma$	8	$3.8 \pm 0.8 \pm 1.5$	$4.2 \pm 2.9 \pm 1.5$	4.6 ± 0.4
$W(\mu\nu)\gamma$	5	$2.4 \pm 0.4 \pm 0.9$	$2.6 \pm 2.3 \pm 0.9$	2.5 ± 0.2
$Z(ee)\gamma$	2	$0.3 \pm 0.1 \pm 0.1$	$1.7 \pm 1.4 \pm 0.1$	1.2 ± 0.1
$Z(\mu\mu)\gamma$	2	$0.1 \pm 0.1 \pm 0.1$	$1.9 \pm 1.4 \pm 0.1$	0.7 ± 0.1

The largest photon background in the $W\gamma$ and $Z\gamma$ events is due to a QCD jet that fakes a photon. This is determined using a multi-jet ($n$jets ≥ 3) data sample, in which two highest E_T jets are required to be kinematically similar to jets from hadronic $W(Z)$ decay and the other jets are tested if they pass all photon selection cuts. The probability for a jet to fake a photon was estimated to be ~ 0.002. The systematic uncertainty on this QCD-jet background, which dominates the systematic error in the background estimation, was derived from the difference between the QCD-jet background estimated from the multi-jet sample and that obtained using the $W/Z+$ $n$jets($n \leq 2$) Monte Carlo events generated by the VECBOS+Herwig+CDF detector simulation. Other backgrounds to the $W\gamma$ signal include $Z + \gamma$ (or fake γ), where one of the leptons from Z decay is not detected, and $(W \rightarrow \tau\nu) + \gamma$ (or fake γ). Table 4 summarizes $W\gamma$ and $Z\gamma$ results together with the Standard Model predictions. Combining the electron and muon samples CDF measures $\sigma Br(W(\ell\nu)\gamma) = 17.9^{+11.1}_{-10.7}(stat. \oplus sys.)$ pb and $\sigma Br(Z(\ell\ell)\gamma) = 9.2^{+5.2}_{-5.1}(stat. \oplus sys.)$ pb, where ℓ is e or μ. By comparing the $\sigma Br(W(\ell\nu)\gamma)$ measurement with the predictions obtained using an event generator written by Baur and Zeppenfeld[16] CDF sets limits on anomalous $WW\gamma$ couplings of $-6.5 < \Delta\kappa(= \kappa - 1) < +6.9$ ($\lambda = 0$) and $-3.1 < \lambda < +3.1$ ($\Delta\kappa = 0$) at the 95% CL.

DØ searched for $W(e\nu)\gamma$ events in the 14.5 pb^{-1} inclusive electron W sample by requiring an additional well-measured and isolated photon with $E_T^\gamma \geq 10$ GeV and $\Delta R_{e\gamma} > 0.7$. Both an electron and a photon were required to be in the region of $|\eta| \leq 1.1$. A photon candidate must have an EM cluster satisfying the same quality cuts for electrons described above, but with no 3-D tracks pointing at it. The overall efficiency for a photon is determined to be 0.80 ± 0.04 including the probability of losing a photon due to overlap between random tracks and the EM cluster and the probability of the photon conversion in the material before the calorimeter.

DØ observed 12 $W(e\nu)\gamma$ candidates, 10 events with no jets, requiring E_T(jet) $\geq$ 15 GeV, and 2 events with 1 jet. The QCD-jet background is estimated by taking the E_T distribution of jets in $W + 1$ jet and $W + 2$ jets in the inclusive W sample

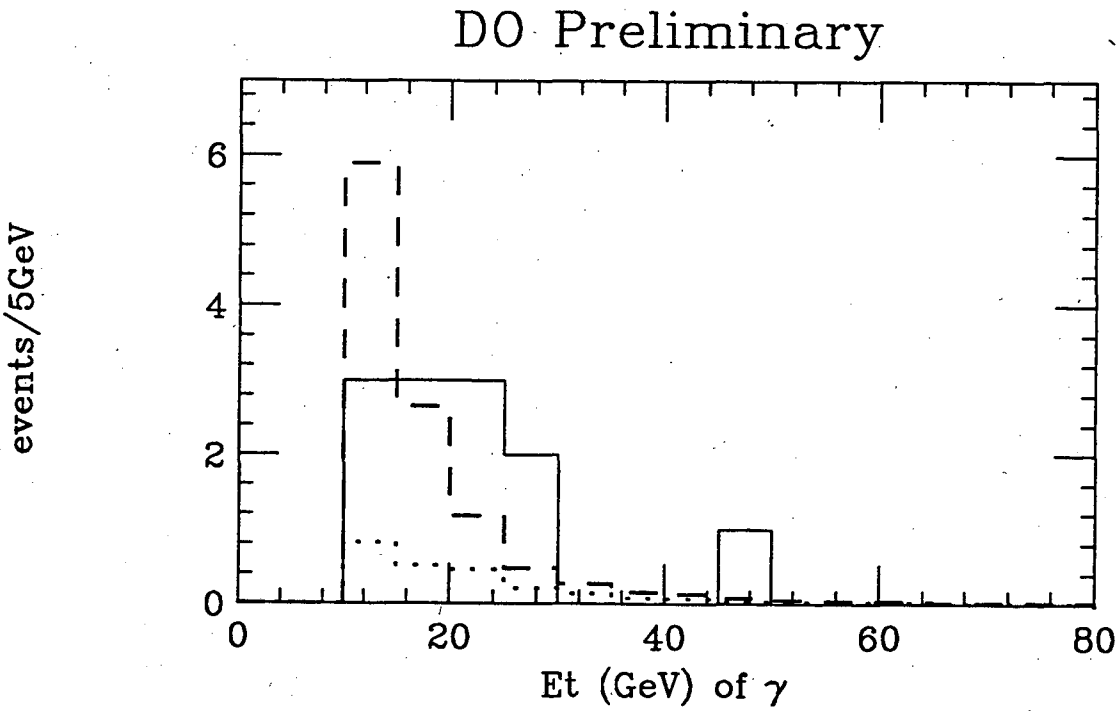

Figure 8: E_T distributions of photons (solid line) in $W\gamma$ candidates from DØ with estimated fake photons (dotted line) and the Standard Model prediction (dashed line).

and multiplying by the probability for a jet to fake a photon. This probability is estimated by counting the number of jets passing all photon selection cuts in a dijet sample and is found to be $(1.0 \pm 0.4) \times 10^{-3}$. The error includes the systematic error due to the presence of direct photon events in a dijet sample. The E_T distribution of photons in the 12 $W\gamma$ candidates is shown in Fig. 8 with the estimated QCD-jet background distribution. The integral of the QCD-jet background distribution gives 2.1 ± 1.0. Other backgrounds including $(W \rightarrow \tau\nu) + \gamma$ (or fake γ) and $Z + \gamma$ (or fake γ), where one of electrons from Z decay is not detected, amount to ~ 0.5 events. The Monte Carlo using a $W\gamma$ event generator by Baur and Zeppenfeld and a fast detector simulator predicts the number of events as $8.5 \pm 1.0 \pm 1.0$ for the Standard Model, where the first error is due to systematic errors in efficiencies and the second due to the systematic error in luminosity estimate. The E_T distribution of photons in the Standard Model prediction is shown in Fig. 8. The Standard Model prediction with the estimated background is consistent with the observed number of events. Work is in progress to extend these studies to larger rapidity region, to include the muon channel and to determine values for the anomalous couplings.

CDF found one WZ pair candidate from the 1992-1993 run. The event consists of 3 isolated electrons with $E_T = 55.5$, 33.7, and 22.2 GeV. Two highest E_T electrons in the central calorimeter are consistent with electrons from $Z \rightarrow ee$ and combining

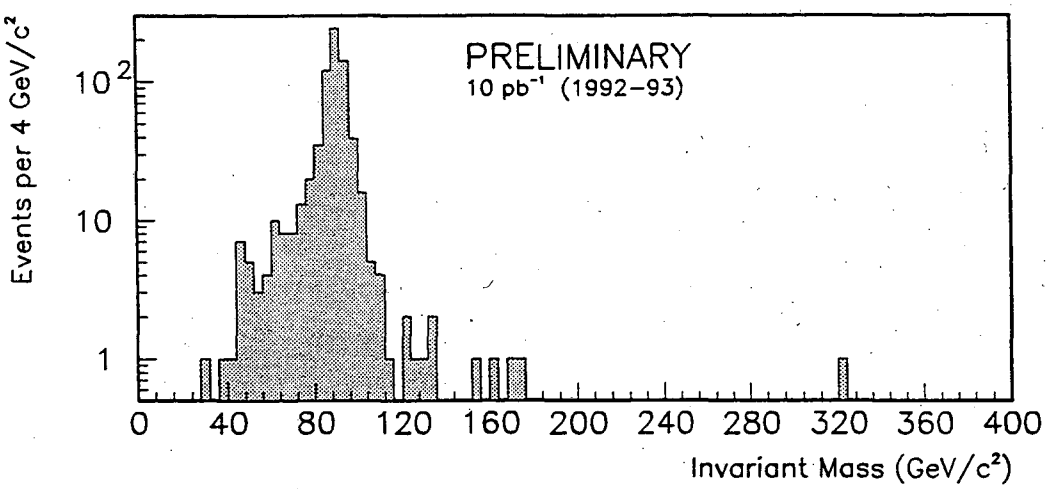

Figure 9: Invariant mass distribution of e^+e^- pairs detected by CDF in ~ 10 pb^{-1} data from the 1992-1993 run.

the 3rd electron in the plug calorimeter with $\not\!\!E_T$forms $M_T > 40$ GeV/c^2. Further study of the event is under way.

7 A search for a new neutral gauge boson (Z')

Neutral gauge bosons in addition to the Z^0 are expected in many models which enlarge the electroweak gauge group beyond the $SU(2)_L \otimes U(1)_Y$ of the Standard Model. These models include left-right symmetric models and grand unified theories. In $\bar{p}p$ collisions these new neutral gauge bosons (Z') can be directly observed via their decay to lepton pairs. CDF set a limit of $M_{Z'} > 412$ GeV/c^2 (95% C.L.)[17] based on a search for $Z' \rightarrow ee$ and $\mu\mu$ in the 1988-1989 data, corresponding to an integrated luminosity of 4.05(3.54) pb^{-1} for the electron (muon) channel. The invariant mass distribution of e^+e^- pairs detected by CDF in ~ 10 pb^{-1} data from the 1992-1993 run is shown in Fig. 9. The sample was selected from events containing at least one central electron with $E_T > 20$ GeV and by requiring an additional central ($E_T > 20$ GeV) or plug ($E_T > 15$ GeV) electron. CDF observed one event ($M_{ee} = 320$ GeV/c^2) above $M_{ee} = 200$ GeV/c^2, consistent with the expected contribution of 1.5 events from the Standard Model Drell-Yan process. The work to extract a new limit is in progress.

8 Conclusion

Preliminary results on electroweak physics from the 1992-1993 Tevatron run with the CDF and DØ detectors were shown. Each detector collected more than 10000 $W \to e\nu$ and more than 1000 $Z \to ee$ events. CDF collected ~ 7600 $W \to \mu\nu$ and ~ 710 $Z \to \mu\mu$ events, while DØ collected ~ 3000 $W \to \mu\nu$ and ~ 200 $Z \to \mu\mu$ events. Using the full electron data sample CDF obtained a new measurement of $\Gamma(W) = 2.033 \pm 0.069(stat.) \pm 0.057(sys.)$ GeV/c^2 and set a limit on the top-quark mass independent of decay mode of $M(t) > 62$ GeV/c^2 at 95% CL. DØ obtained a measurement of $\Gamma(W) = 2.08 \pm 0.25(stat. \oplus sys.)$ GeV/c^2 and set a top quark mass limit of $M(t) > 43$ GeV/c^2 combining electron and muon channels, based on a partial data sample. CDF expects to improve its measurement of the charge asymmetry of electrons from the W decay. Taking advantage of this high statistics W and Z data sample, preliminary results on the $W\gamma$ production at DØ and on WZ diboson production at CDF were obtained. Measurements of the $W\gamma$ and $Z\gamma$ productions at CDF from the previous run were also presented.

The author is grateful to the conference organizers for their hospitality, and is indebted to experimental colleagues at DØ for their help in preparing the talk. Special thanks are due to Drs. S. Eno and J. Proudfoot for providing CDF results. The author also expresses his gratitude to the technical staff at Fermilab for their excellent support.

References

[1] CDF member institutions include Argonne National Laboratory; Brandeis university; Istituto Nazionale di Fisica Nucleare (University of Bologna); University of California at Los Angeles; University of Chicago; Duke University; Fermi National Accelerator Laboratory; Laboratori Nzionale di Frascati; Harvard University; University of Illinois,Urbana; Institute of Particle Physics (McGill University); The Johns Hopkins University; National Laboratory for High Energy Physics (KEK); Lawrence Berkeley Laboratory; Massachusetts Institute of Technology; University of Michigan; Michigan State University; University of New Mexico; Osaka City University; Universita di Padova; University of Pennsylvania; University of Pittsburgh; Istituto Nazionale di Fisica Nucleare (University and Scuola Normale Superiore of Pisa); Purdue University; University of Rochester; Rockfeller University; Rutgers University; Superconducting Super Collider Laboratory; Texas A&M University; University of Tsukuba; Tufts University; University of Wisconsin and Yale University.

[2] DØ member institutions include Universidad de los Andes (Colombia); University of Arizona; Brookhaven National Laboratory; Brown University; University

of California, Riverside; Centro Brasileiro de Pesquisas Fisicas (Brazil); CINVESTAV (Mexico); Columbia University; Fermi National Accelerator Laboratory; University of Florida; Florida State University; University of Hawaii; University of Illinois, Chicago; Indiana University; Iowa State University; Lawrence Berkeley Laboratory; University of Maryland; University of Michigan; Michigan State University; Moscow State University (Russia); New York University; Northeastern University; Northern Illinois University; Northwestern University; University of Notre Dame; University of Panjab (India); Institute for High Energy Physics (Russia); Purdue University; Rice University; University of Rochester; DAPNIA-CE Saclay (France); State University of New York,Stony Brook; Superconducting Supercollider Laboratory; Tata Institute of Fundamental Research (India); University of Texas, Arlington; Texas A&M University and ZRL.

[3] CDF Collab., F. Abe *et al.*, Nucl. Instrum. and Methods, Phys. Res., Sect. **A271**, 387 (1988).

[4] DØ Collab., S. Abachi *et al.*, submitted to Nucl. Instr. and Meth. in Phys. Research **A**.

[5] CDF Collab., F. Abe *et al.*, Phys. Rev. **D44**, 29 (1991).

[6] UA1 Collab., C. Albajar *et al.*, Phys. Lett. **B198** (1991)503; UA2 Collab., J. Alitti *et al.*, Phys. Lett. **B276** (1991)365; CDF Collab., F. Abe *et al.*, Phys. Rev. Lett. **64**, 152 (1990); CDF Collab., F. Abe *et al.*, Phys. Rev. Lett. **69**, 28 (1992).

[7] W. F. L. Hollik, Fortschr. Phys. **38**, 165 (1990).

[8] The LEP Collaborations: ALEPH, DELPHI, L3 and OPAL, Phys. Lett. **B276** (1992) 247.

[9] A. D. Martin, W. J. Stirling and R. G. Roberts, Phys. Lett. **B228** (1989)149.

[10] R. Hamberg, W. L. van Neerven and T. Matsuura, Nucl. Phys. **B359** (1991)343.

[11] NMC Collab., D. Allasia *et al.*, Phys. Lett. **B249** (1990) 366; P. Amaudruz *et al.*, Nucl. Phys. **B371** (1992) 3.

[12] T. Alvarez, A. Leites and J. Terrón, Nucl. Phys. **B301** (1988)1.

[13] E. L. Berger, F. Halzen, C. S. Kim and S. Willenbrock, Phys. Rev. **D40**, 83 (1989).

[14] A. D. Martin, R. G. Roberts and W. J. Stirling, Mod. Phys. Lett. **A4**, 1135 (1989).

[15] UA2 Collab., J. Alitti *et al.*, Phys. Lett. **B277**(1992)194.

[16] U. Baur and E. L. Berger, Phys. Rev. **D41**, 1476 (1990).

[17] CDF Collab., F. Abe *et al.*, Phys. Rev. Lett. **68**, 1463 (1992).

LAWRENCE BERKELEY LABORATORY
UNIVERSITY OF CALIFORNIA
TECHNICAL INFORMATION DEPARTMENT
BERKELEY, CALIFORNIA 94720